CrossMark

Electroactive nanostructured scaffold produced by controlled deposition of PPy on electrospun PCL fibres

Sajjad Shafei[1] · **Javad Foroughi**[2] · **Leo Stevens**[2] ·
Cynthia S. Wong[1] · **Omid Zabihi**[1] · **Minoo Naebe**[1]

Abstract The electrical conductivity of biodegradable polymeric scaffolds has shown promising results in tissue engineering, particularly for electrically excitable tissues such as muscles and nerves. Herein, we demonstrate a novel processing approach to produce electroactive nanofibres. Electrically conducting, robust nanofibres comprising both a biodegradable component using poly(ε-caprolactone) (PCL) and a conducting component, polypyrrole (PPy), have been produced by electrospinning and vapour phase polymerization. The PCL/PPy nanofibres were characterised in terms of morphology, electrical conductivity, and dimensional stability. The as-prepared nanofibres were found to be cytocompatible with good electrical conductivity and mechanical properties. It was found that electrical conductivity of the PPy coated PCL nanofibre was 1.9 S/cm, which is much higher than that of PCL mixed with PPy in other studies. Cell viability on the scaffolds were firstly examined by in vitro culturing the L929 fibroblast cells for 24 h, revealing viability of 97.6 ± 2.7 %. Then PC12 cells differentiation observed by neurite outgrowth which occurred after 4 days of culture on the scaffolds. Significantly larger areas of the PPy coated PCL were covered by cells compared to PCL without coating. The obtained results from filament staining suggested the high potentials of the conducting scaffold for use in neural tissue engineering.

✉ Minoo Naebe
  minoo.naebe@deakin.edu.au

[1] Institute for Frontier Materials, Deakin University, Geelong, Australia

[2] Intelligent Polymer Research Institute, University of Wollongong, Wollongong, Australia

🍬 Springer

Introduction

Synthetic biodegradable polymers such as poly(lactic acid) (PLA), poly(glycolic acid) (PGA), and poly(ε-caprolactone) (PCL) are increasingly being employed in tissue engineering applications due to their high controllable physical properties [1]. For tissue engineering applications, polymeric scaffolds are ideally supportive of cell growth, mechanically robust, undergo controlled biodegradation and are ultimately excreted by the lymphatic system with no toxic by-products [2]. PCL is particularly promising, having a slow degradation rate, exceptional mechanical properties and widely reported cytocompatibility whilst being one of the least expensive options among the biodegradable polymers [3]. Electrospun fibre-based scaffolds have shown outstanding results due to their similarities to the fibrous extracellular matrix (ECM) [4], and electrospun PCL fibres have been investigated for many different tissue engineering applications, including cartilage, bone, cardiac, and nerve tissue engineering [5–7]. The benefits of electrospinning are particularly apparent in neural tissue engineering, as electrospinning forms fibrous scaffolds that can guide and support neuron extension [8]. For example, rat Schwann cell line (CRL-2765) cultured on random and aligned electrospun PLGA–PCL demonstrated better axonal growth on the aligned nanofibres [9]. Additionally, PCL is highly blend-compatible, and great effort has been devoted to fabrication of blended PCL scaffolds [10–12]. Gelatin as a natural polymer has been blended in different ratios with PCL to produce nanofibres, which were employed for the in vitro culture of neural stem cells (PC17.2 cells) [13].

Because of the responsive nature of some tissues to electrical signals, conducting scaffolds has been extensively studied [12, 14]. Conducting polymers such as polypyrrole (PPy), polythiophene (PTh), and polyaniline (PANI) have the advantages of both metals and polymers in that they have superior electrical and optical properties in addition to flexibility in process and synthesis [15–17]. Conducting polymers as coating have mostly been produced either electrochemically or chemically, although enzyme catalysed and photochemically initiated polymerisation also have been investigated [18, 19]. Vapour-phase polymerisation, which is a chemical deposition method, can help control the thickness of the coatings and where needed, coat in the range of nanometre thickness [20, 21]. PPy has one of the highest conductivities among these polymers, with a good chemical stability in air and water [18]. PPy has been reported to have 1.5 GPa elastic modulus, but a brittle structure breaking with 2 % elongation at 25 MPa tensile strength [22]. Additionally, PPy is the most investigated conducting polymer for biomedical applications, especially as a copolymer, or in blends and composites with various biocompatible and biodegradable polymers [23]. For example, a particle composite of PCL–PPy developed using emulsion polymerisation showed improved mechanical properties [24]. Many cell types including neural, bone, and glial cells have shown biocompatibility with PPy [25]. Aligned PPy fibres have been reported to introduce orientation in neurites of PC12 cells with the cells proliferating in parallel to the fibres on a scaffold [26]. On the other hand, it is possible to make conducting polymers degrade when synthesised in a mixture consisting of biodegradable

polymers [18, 27]. Thus, using conducting polymers, a number of scaffolds for bone [28], muscle [29], cardiac [30], and nerve [31] tissue engineering have been fabricated to be conducting and biodegradable. In a study by Kai et al. [30], membranes made up of PPy, PCL, and gelatin were fabricated and characterised. The electrospun fibres containing 15 % PPy were reported to be a good candidates due to mechanical stability and degradation rate being matched with cardiac tissue regeneration. However, as PPy is embedded into the fibres, the conductivity is almost 10^4 times (0.01–0.37 mS/cm) less than fibres with PPy coated on the surface, which implies that to have higher conductivities, surface coating of conducting polymers is more efficient than mixing. For neural tissue engineering in particular, culturing of PC12 cells along with stimulation of the conducting scaffolds has been widely studied using direct and alternative currents [31–34]. Lee et al. reported a conducting electrospun scaffold using PLGA coated by PPy. Surface resistivity in their scaffold ranged from 3 kΩ/sq to 0.7 MΩ/sq. The cell attachment and differentiation of electrically stimulated PC12 cells showed 40–50 % longer neurites and 40–90 % higher neurite formation compared to the unstimulated cells, while a 2-week stability test resulted in only a little delamination and fragmentation of the PPy shell [35]. However, all of these methods coat the entire scaffold with the conducting polymer, while a scaffold with surface coating can still provide the conducting substrate to transmit signal between the cells.

In this study, we have developed a novel method to fabricate electroactive PCL nanofibre mats with the potential of using it for nerve and muscle tissue engineering. Electrospraying and vapour-phase polymerization instead of the conventional dip coating method was employed to provide better control for the deposition of PPy. This technique produced a conductive scaffold by only coating the surface of the membrane with the conducting polymer. Cytotoxicity of the membrane was tested using fibroblast cells to demonstrate cell viability on the developed membrane. PC12 cells seeded onto the scaffold to demonstrate potential applications of this membrane as a nerve tissue engineering scaffold.

Materials and methods

Materials

Poly(ε-caprolactone) (PCL Mn = 80 kDa), pyrrole, Dimethylformamide (DMF), Tetrahydrofuran (THF) and n-butanol were purchased from Sigma-Aldrich. We obtained 40 wt% ferric p-toluene sulphonate $Fe(Tos)_3$, also known as Fe.pTS, in n-butanol from Heraeus Deutschland GmbH & Co.

Fabrication of electrospun nanofibre

After optimizing electrospinning and electrospraying parameters, 14 wt% PCL was dissolved in DMF:THF with volume ratio of 1:1 using a magnetic stirrer at 50 °C overnight. A 5-cm diameter drum rotating at a speed of 2 rev/s was used to collect fibres that were homogenously distributed on the perimeter of the drum. The

electrospinning followed by electrospraying of the oxidant on the drum rotating at the same speed. The Fe.pTS as oxidant was diluted to 4 % concentration in n-butanol to be sprayed on the collector covered with an electrospun fibre mat of PCL. Five samples were prepared with different amounts of electrosprayed oxidant. A control sample of pure PCL with no electrospray deposition or coating was compared with four samples exposed to 1, 2, 3, and 4 h of oxidant electrospraying. Given the distribution geometry of the oxidant, an approximate 17 µmol/cm^2 oxidant has been electrosprayed every hour. Figure 1 illustrates the process and specifications of the samples.

Immediately after electrospraying each sample, vapour-phase polymerisation of pyrrole took place. Fibre mats were detached from aluminium foil and cut into dimensions of 16×10 cm^2. Samples were placed in an airtight chamber containing 1 mL pyrrole as the monomer of PPy at room temperature. The monomer dropped and flowed onto a watch glass exposing approximately 3 cm^2 liquid surface into a 1 L volume. After 1 h of vapour phase polymerisation in the chamber, the surface of the fibre mats turned black. Once the polymerisation completed, specimens were well washed using methanol and water and dried at room temperature.

Morphology

SEM images were taken from the surface of the fibre mats using Zeiss Supra 55VP. In order to perform conductivity analysis, the thickness of coatings was measured. Assuming that the PPy coating around each fibre section is almost uniform, it is possible to find the thickness of the coatings of polypyrrole. The proportion of the coated area to the entire sample was measured by "MinError" method in ImageJ software.

The porosity of the membranes was estimated using gravimetric analysis. The bulk volume of the fibre mats was determined using five samples of 3×3 cm^3 and

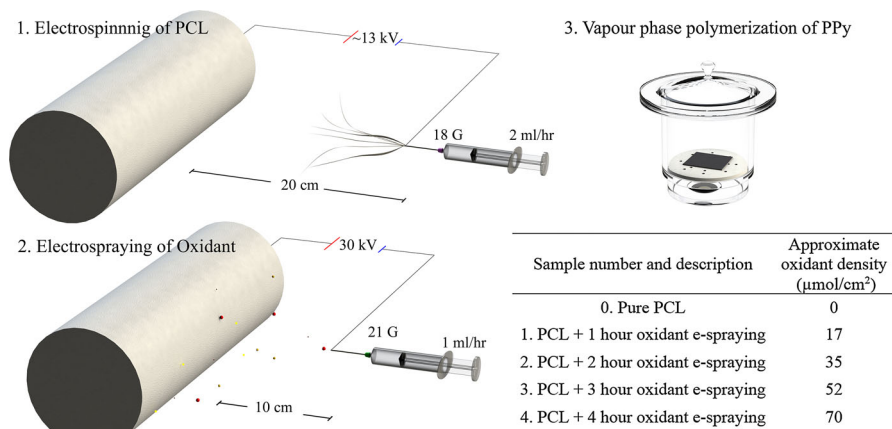| Sample number and description	Approximate oxidant density (µmol/cm²)
0. Pure PCL	0
1. PCL + 1 hour oxidant e-spraying	17
2. PCL + 2 hour oxidant e-spraying	35
3. PCL + 3 hour oxidant e-spraying	52
4. PCL + 4 hour oxidant e-spraying	70

Fig. 1 Schematic presentation of the fabrication process. PCL fibres electrosprayed by Fe.pTS which followed by polymerisation of PPy using pyrrole as the monomer in an airtight chamber

by measuring their thickness. The skeletal volume of the meshes (which represent the membranes with no pore) was calculated by converting the measured mass of the samples to volume using the polymer density. This measurement, which only applied to the control sample, can estimate the inside porosity of the samples. On the other hand, to estimate the surface porosity appropriate for cell attachment SEM images were analysed. Using ImageJ software, the pore threshold recognition were employed using "Moments" method.

Electrical conductivity

Electrical resistivity was measured according to the AATCC 76-2011. Briefly, conditioned samples were cut into specimens of 3×1 cm^2 in the 4th week after fabrication for stabilisation purposes [36]. Five samples in each direction were prepared. Two clean copper probes each with size of 1×1 cm^2 used in a fixed setup being able to enfold the specimens. By the requirement of the standard the pressure applied on the probes was increased until it did not affect the results. An approximate force of 1.2 N was applied on each probe, which is close to other measurements performed by this method [37]. The 1×1 cm^2 gap in the centre, was left between the probes to conduct electricity. The probes was connected to a multimeter (Fluke 189) for resistivity measurements. Almost three significant figures were readable regardless of the order of resistivity.

Dimensional stability

Tensile testing of the fibre mats was performed using 30×10 mm^2 samples. A surgical blade was used to cut the samples in two directions. The thickness of the fibre mats was measured before cutting the specimens by a fabric thickness tester under 0.5 kPa pressure to give a reproducible estimation of the thickness for stress calculations. The top and bottom edges of the specimens were stuck down using a narrow tape. This was to ensure that the specimens did not slipped into the jaws of the instrument during the test. One cm from either sides of the specimens was placed into each jaw tightened by pneumatic pressing force and gauge length of 10 mm was selected. Specimens encountered a gentle pre-test load to ensure measurements are done after the mats straightened. An Instron tensile tester (100 N load cell) applied an elongation with a constant rate of 50 mm/min.

Thermogravimetric analysis was carried out using a Q50 TGA (TA Instruments). PCL/PPy samples were heated with 10 °C/min from room temperature to 500 °C under a nitrogen gas flow of 60 mL/min (balance gas 40 mL/min).

Differential scanning calorimetry was conducted using a Q200 DSC (TA Instruments). Samples were heated with 10 °C/min from −80 to 300 °C.

Cell culture

PCL-PPy membranes were tested for their cytocompatibility and ability to support the growth of two cell lines, L929 mouse fibroblasts and PC12 neuronal rat pheochromocytomas (American Type Culture Collection). Four-well Labtek-II

chamber slides (Thermo Fisher Scientific) were separated from their glass bases, which were then replaced with PCL–PPy or uncoated PCL membranes supported on microscope slides and sealed using silicon adhesive (Permatex). After allowing 12 h for complete setting, all wells were washed three times with reverse osmosis H_2O, transferred to a sterile biosafety cabinet (BSC) and then sterilised with 70 % ethanol. Each well was then filled with Dulbecco's Modified Eagle Medium (DMEM, Invitrogen) and incubated overnight at 4 °C.

Growth media was prepared for L929 [DMEM + 10 % foetal bovine serum (FBS, Invitrogen)] and PC12 [DMEM + 5 % FBS, + 10 % horse serum (HS, Sigma)] cells, and brought to 37 °C. Populations of L929 and PC12 cells were then seeded into the Labtek wells at 4×10^3 cells/cm^2, in their respective growth media and incubated in a humidified environment at 37 °C and 5 % CO_2. After 24 h in growth media, PC12 cells were cultured in differentiation media [DMEM + 1 % HS +50 ng/mL nerve growth factor (NGF, Life Technologies)] and allowed to differentiate for a further 4 days with a media change after 2 days. At the same 24 h time point, L929 cells were assessed for viability by staining with calcein AM (Molecular Probes, Life Technologies) and propidium iodide (PI, Sigma) in phosphate buffered saline (PBS). Stained cells were visualised using an Axioimager fluorescence microscope (Zeiss) and cell viability was quantified by Metamorph image analysis software (Molecular Devices).

After 4 days of differentiation, PC12 cells were immunostained for the key differentiation marker ß-III tubulin, as well as nuclear stained with DAPI. Media was removed from wells and replaced with 50:50 methanol:acetone on ice for 5 min to permeabilise cells, which were then washed with PBS and blocked in 10 % donkey serum (DS, Chemicon) with 0.05 % Tween-20 (Sigma) for 1 h at 21 °C. Cells were then exposed to the primary antibody (anti-ß-tubulin, Covance) and diluted 1:1000 in blocking solution overnight at 4 °C. After two 10 min washes in PBS, cells were incubated for 1 h at 21 °C in the dark with the secondary antibody Alexa-546 donkey anti-mouse (Invitrogen) diluted 1:1000 in blocking solution. During the second of three 10-min washes in PBS, DAPI (Molecular Probes) was added at 1:1000 in PBS for 5 min at 21 °C before replacing with fresh PBS and imaging on the Axioimager fluorescence microscope.

The morphology of PC12 cells were observed by SEM. Cells cultured on various membranes were fixed in 4 % paraformaldehyde for 10 min. The cell-seeded membranes were then dehydrated increasing concentrations of ethanol (25, 50, 70, 90, 100 %, and again 100 %, for 5 min each). Approximately 6 mm^2 cell cultured area from samples analysed to evaluate the cell coverage on each scaffold.

Statistical analysis

Statistical analyses were carried out using SPSS 22.0 for Windows. Values are represented with the format of mean ± standard deviation. Mean comparison were performed using one-way analysis of variance (ANOVA) and Duncan's method to classify samples in subsets. Significance level of $p \leq 0.05$ were used in the analysis.

Results and discussion

Morphology

Figure 2 shows the SEM images of the control and coated samples. As expected, increase of the electrospraying time leads to increase in the coated area of PCL by PPy. An estimation of the proportion of the coated area to the total area in addition to the thickness of the coatings deposited on the surface of the fibres are presented in Fig. 2f. As shown in Fig. 2f, electrospraying oxidant for 4 h produced cracks on the membrane. This was most likely due to the brittle nature of PPy [18].
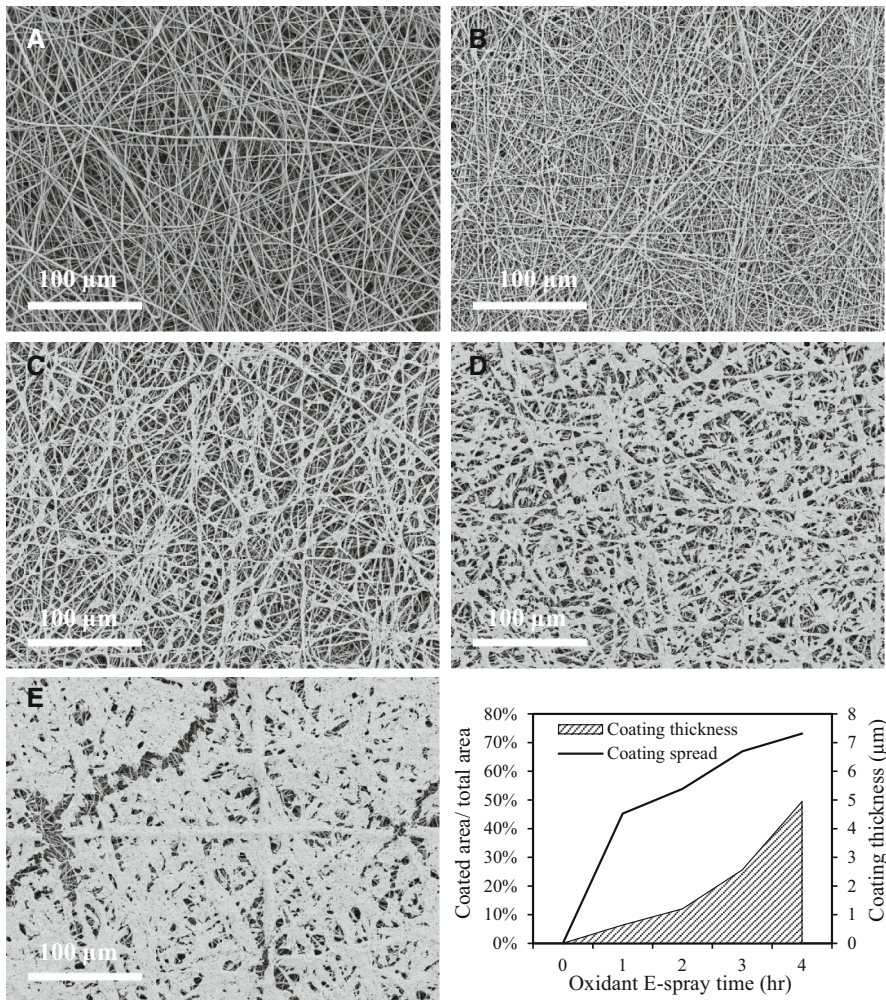
Fig. 2 SEM images of electrospun fibres of PCL and PPy coated PCL. Sample number 2 had 54 % coating spread and 1.2 μm coating thickness. **a** PCL fibre mat without coating, **b** 1 h oxidant electrospray, **c** 2 h oxidant electrospray, **d** 3 h oxidant electrospray, **e** 4 h oxidant electrospray, **f** coating thickness and spread

This method demonstrated a uniform distribution of the PPy coating (Fig. 2 image c, d, and e). The cracks observed in Fig. 2f under SEM microscopy can be considered a major disadvantage for further use of PPy. In this sample, small layers of PPy (e.g. 1 mm^2) can be removed by forces applied to the surface of the fibre coatings. The vulnerability observed in these coatings led to 5 μm being designated as the maximum PPy thickness used for coating in this experiment.

Samples analysed at a higher magnification using SEM are demonstrated in Fig. 3. For PCL fibres before coating, fibre diameter measured showed a mean of 0.87 ± 0.42 μm for 100 measurements (Fig. 3a).

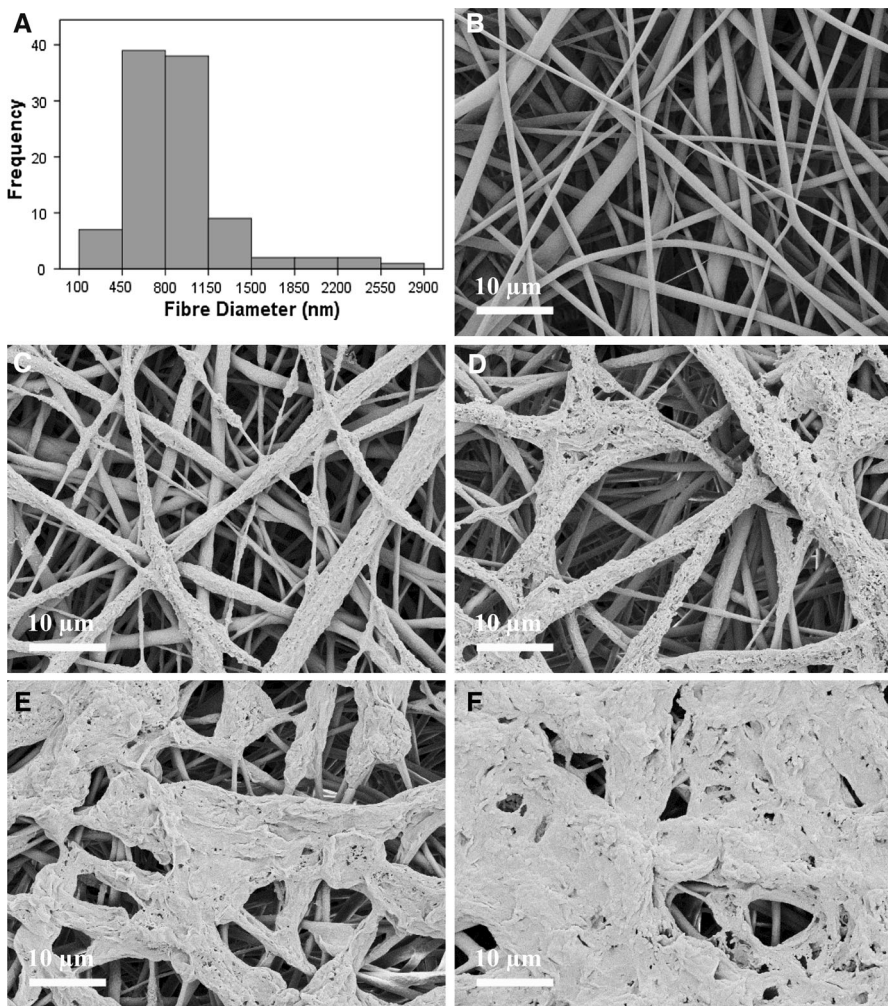Fig. 3 High magnification SEM images of electrospun fibres of PCL and PPy coated PCL. a Fibre diameter distribution, b PCL fibre mat without coating, c 1 h oxidant electrospray, d 2 h oxidant electrospray, e 3 h oxidant electrospray, f 4 h oxidant electrospray

SEM images b–f shown in Fig. 3 demonstrate that electrospraying time of the oxidant is a significant factor in defining several parameters of the membrane as the PPy surface coating increases. The present study used a 2 mL/h production rate, which is higher than a similar study with 14 % PCL in DMF:THF (1:1) [7]. The fibre diameter has a diverse distribution, which can be beneficial in cell culture as evidenced in a study by Kim et al. [38] describing a nano- and micro-scale fibre composition. Fibres produced in this study has a wide range of diameter distribution from 100 nm to 3 μm. The presence of nanofibres in the structure of the scaffolds can lead to enhanced cell growth [39], while microfibres can result in larger pores, which allows better gas and nutrient exchange [38].

The PPy coating has changed the morphology of the round PCL fibres to a rough surface full of nanoscale pores, grooves, and jagged features. Figure 4 shows the surface morphology of the coated fibres. In one study, cell growth was enhanced when cultured on grooved fibres compared to round fibres [40]. Higher surface area and use of grooves on the fibres improved the proliferation of the cells [41]. The smooth surface of the PCL fibres shown in Fig. 4a changed to a jagged surface as in Fig. 4b with a higher potential for cell attachment.

The effect of electrospraying time on the porosity and surface porosity of the fibre mats are also presented in Fig. 5. The inner porosity was measured for the control sample and applied to all samples as the inner porosity of all samples were designed to be similar. The average inner porosity was 91.9 ± 0.2 %, which was measured in five samples. The surface porosity were measured using SEM images. The results showed a gradual decrease in the surface porosity of the fibre mats with the increase in electrospraying time.

The inner porosity of approximately 92 % demonstrated in these scaffolds meets the typically stated requirement of 90 % porosity for tissue engineering [42, 43]. A study on peripheral nerve regeneration showed that scaffolds with 80 % inner porosity were able to support nerve regeneration [44]. However, the reduction of the surface porosity can have two conflicting effects. First, because of the higher surface conductivity, it can result in enhanced cell signalling and consequently better cell
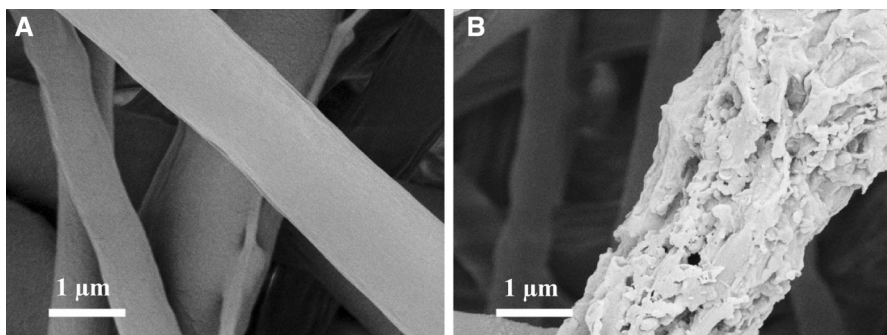

Fig. 4 PCL fibres in image **a** has found nanoscale features by PPy coating in image **b,** which resulted in a jagged surface with better supports for cell attachment. Indentations, pores, and grooves can enhance the growth of the cells attached to the coated fibres. **a** PCL fibres without PPy coating, **b** PPy coated PCL fibres with 2 h oxidant electrospray

Fig. 5 Porosity and surface porosity measurement at various electrospraying times
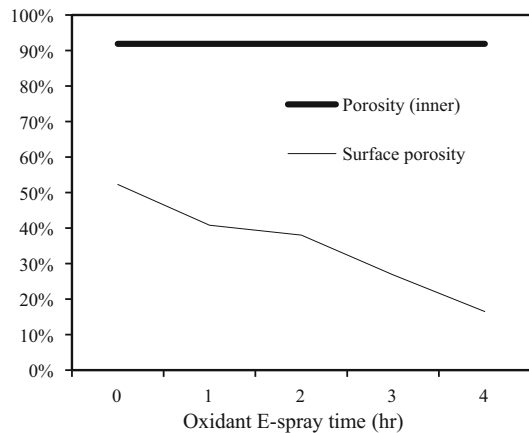
growth [31, 45]. On the other hand, as the porosity decreases, flow of nutrients will become less effective. In a 7-day cell culture study of human bone cells, cells penetrated into the electrospun fibre mat with 30–53 % surface porosity [46]. A minimum of 17 % surface porosity of samples in the present study can still be used for cell culture as a finite element optimisation states at least 5–15 % surface porosity is a prerequisite for the scaffolds [47].

Electrical conductivity

The main interest for use of PPy in the scaffold is stimulation of electrically excitable cells as the current passes through the substrate for cells to grow. The results of the surface electrical resistivity of the fibre mats are presented in Fig. 6. The difference between needle and perpendicular direction is not statistically significant. Duncan's ANOVA tests, categorises the sample number 3 and 4 in the same group as shown in Table 1. This is mainly because of the minute cracks on the surface of the sample number 4. In this sample, although thicker and more universal coatings of PPy have provided a wider passage for electricity conduction, random cracks have changed the electron traffic to abundant stops. As no further conductivity was expected with higher use of PPy, 4 h of electrospraying PPy with oxidant was fixed as the upper limit for this experiment. Electrospraying for 0.5 h was found to produce a non-conducting surface. Therefore, 1 h of electrospraying PPy was identified as the minimum amount used in this study.

In order to compare the results of this experiment with some other existing studies, the surface resistivity converted to conductivity. To accomplish this goal, conductivity is calculated based on the morphological measurements of coating thickness and spread. The results by exclusion of sample number 4 show the conductivity values ranging from 1.3 to 1.9 S/cm, which is 10^4 times higher than the conductivity of PPy mixed with PCL [30]. Incorporation of a non-conducting polymer in the mixture which may occur along with the shrinkage and phase separation of the components during spinning of polymer blends and formation of
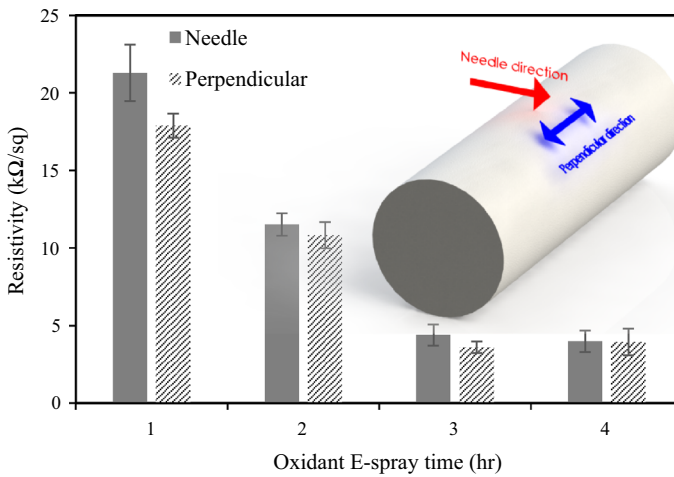
Fig. 6 Surface resistivity of the conducting membranes. Thicker and wider distribution of the PPy coating has increased the conductivity of the samples

Table 1 Duncan's ANOVA analysis of the surface resistivity of the fibre mats. Samples with 3 and 4 h of electrospraying of the oxidant did not show significant difference in conductivity

Oxidant spray time (h)	Needle axis Subset for alpha $= 0.05$			Perpendicular axis Subset for alpha $= 0.05$		
	1	2	3	1	2	3
4	3.9			3.9		
3	4.4			3.6		
2		11.5			10.8	
1			21.2			17.8
Sig.	0.55	1	1	0.48	1	1

Resistivity in (kΩ/sq), uses harmonic mean; Sample size $= 5$. Means for groups in homogeneous subsets are displayed

core–shell structures can explain the significant difference of the conductivities [48–50]. This is while coating of conducting polymers particularly in the way carried out in this study exposes the conducting portion of the fibre for electron transmission. The calculations on sample number 4 do not comply with the rest of samples, apparently because of the surface cracks observed on this sample. This means that part of the coating spread cannot participate in electrical conductivity.

Pure PPy in the best case can possess conductivities ranging from 10^2 to 7.5×10^3 S/cm [18]. The wet-spun PPy fibres were reported to have ~ 3 S/cm conductivity using Di-(2-ethylhexyl) sulfosuccinate dopant anion (fibre diameter of ~ 150 μm) [22]. In another study using vapour phase polymerisation and Fe.pTS, the same oxidant used in this research, PEDOT and PPy showed 1.0 and 0.07 S/cm conductivity, respectively (coating thickness of 5–12 nm) [21]. We have

conductivities ranging up to 1.9 S/cm suggesting that the thicker coatings have prevented potential gaps between PPy coatings.

Dimensional stability

The scaffold must not collapse during surgical implantation. Also, after implantation, the patient's regular activities must not lead to deformation of the scaffold [51]. Dimensional stability can be evaluated by mechanical and thermal performance of the prepared scaffolds. Figure 7 demonstrates the Young's modulus and tensile strength of the fabricated membranes. Statistically significant increase can be observed in the Young's modulus of sample numbers 3 and 4 in Fig. 7a. Figure 7a, b shows higher Young's modulus and higher tensile strength in the perpendicular direction compared to the needle direction, suggesting that the small diameter collecting drum with a low surface speed has formed the fibres mostly in the perpendicular direction. In the modulus, both in the needle and perpendicular directions, samples 3 and 4 showed statistically significantly higher values. In addition to samples 3 and 4, which exhibited more strength, sample 1 showed significantly lower strength compared to the rest of the samples. The elongation at the break of the samples was also observed and analysed. Considering both needle and the perpendicular directions, no constant pattern of changing could be achieved. However, the average elongation at the break in the needle direction is significantly higher than that in perpendicular direction, which was observed to be 500 and 390 %, respectively. These values are significantly higher than fibres produced from PCL dissolved in HFP, which showed about 200 % elongation of the fibres at break [13].

By increasing the alignment of the fibre mats, an elastic modulus of ~ 11.6 MPa could be achieved using 0.5-μm diameter PCL fibres, suggesting that the fibre alignment can be remarkably effective in the modulus [52]. In this study, due to the low linear speed of the collector, the alignment of the fibres is almost unchanged compared to a stationary collector. However, the results show higher modulus and tensile strength in the perpendicular direction. This can be due to the small diameter
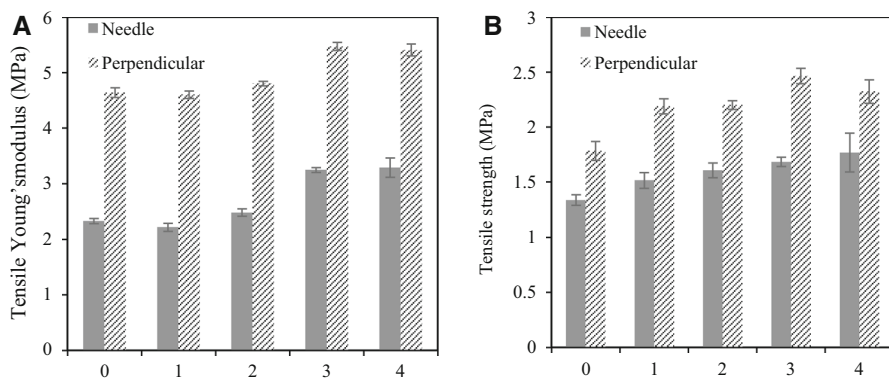

Fig. 7 Mechanical properties of the membranes in tensile testing. **a** Oxidant E-spray time (h), **b** oxidant E-spray time (h)

drum and its low surface speed. PCL fibres with $\sim 600\ \%$ elongation at break and tensile strength of 4.8 MPa were asserted to perfectly meet the mechanical properties required for arterial circulation tissues [53].

The sample electrosprayed for 2 h with oxidant was selected as the sample with the most balanced properties considering the smaller thickness of the coating, electrical conductivity, and mechanical properties. Thus, sample number 2 is used in TGA and DSC tests and for the cell culture analysis. The remaining mass in TGA and the heat flow in DSC are shown in Fig. 8. As can be seen, the PPy coating not only has no adverse effect on the inherent properties of PCL fibres as the base of the scaffold, but also the overall melting point has increased compared to PCL fibres. This means that heat needed to melt and decrystalise the coated samples has increased. Moreover, PPy coated on the PCL increases thermal stability of the scaffold, as evidenced by an increase in initial thermal decomposition temperature. Using the difference between weight losses of samples, it can be also estimated that $\sim 3\ \%$ PPy with respect to the total weight of the scaffold is coated on the structure of the membrane electrosprayed for 2 h with oxidant. This $\sim 3\ \%$ PPy leads to electrical conductivity without sacrificing its porosity.

Cell culture

The ability of the PCL–PPy membranes to support cell growth was initially investigated using the L929 fibroblast cell line. L929 cells seeded onto tissue culture plastic (TCP) as control, PCL, and PCL–PPy sample number 2 and grown for 24 h were stained with the cell viability markers calcein AM. This marker is metabolised by viable cells to form the green-fluorescent calcein molecule, as well as the red-fluorescent propidium iodide, which is excluded by the membranes of viable cells, but enters dead or highly damaged cells. Fluorescence microscopy taken of these L929 cells (Fig. 9a–c) showed a majority of the cells exhibiting green-fluorescence, indicative of high viability across all three of the tested surfaces. The viabilities of L929 cells, as quantified by image analysis were $97.6 \pm 2.7\ \%$ for PCL–PPy,
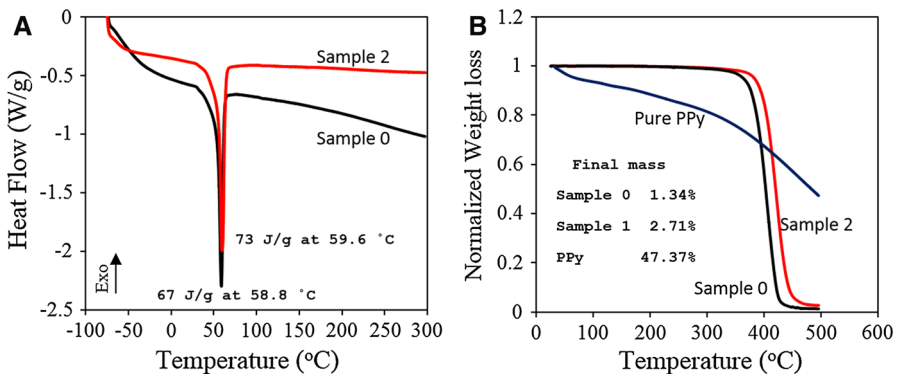

Fig. 8 Differential scanning calorimetry (**a**) and thermogravimetric analysis (**b**) of the samples. TGA results show that the membrane electrosprayed for 2 h with oxidant has approximately 3 % PPy and 97 % PCL in the structure
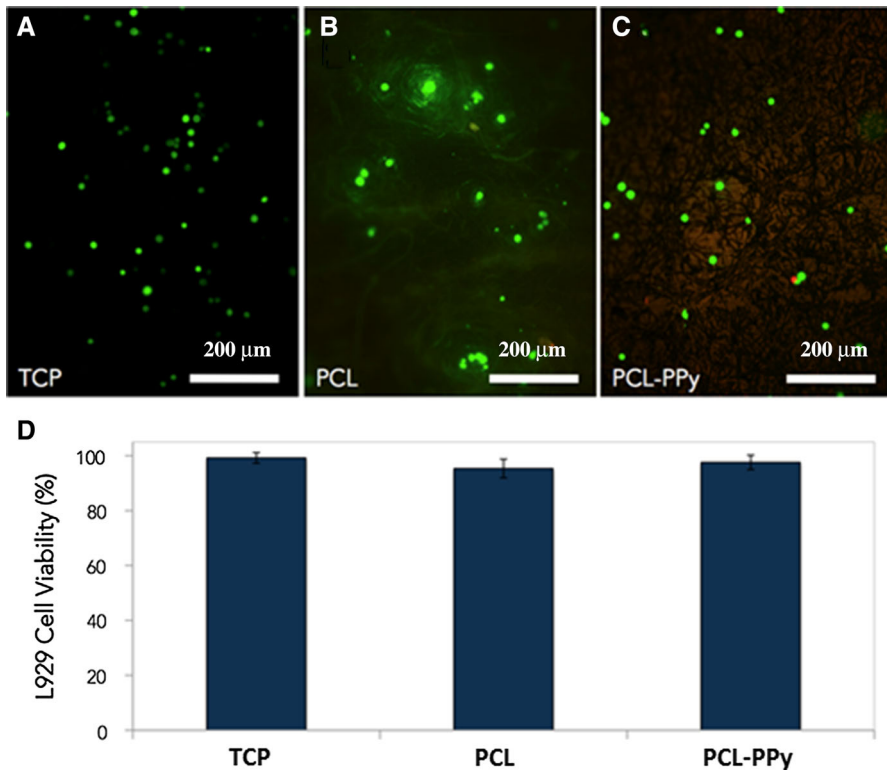
Fig. 9 L929 cells stained with calcein AM (*green*) and propidium iodide (*red*) after 24 h proliferation on TCP (**a**), PCL (**b**), and PCL–PPy (**c**). Viability was quantified for each sample (**d**) by image analysis of the stained L929 cells ($n = 250$–2500). The viability of cells proliferating on PCL–PPy membranes was within ± 1 S.D. of both PCL and TCP controls. (Color figure online)

95.3 ± 3.4 % for PCL membranes without PPy coating and 99.2 ± 1.9 % for TCP controls. These results demonstrated that the PCL and PCL–PPy membranes were not toxic to fibroblasts and, therefore, possess excellent biocompatibility. Consequently, the PCL–PPy membranes were further examined using PC12 cells, a cell line that can be differentiated into nerve-like cells. This enabled the potential of PCL–PPy to be investigated as a biomaterial for its intended application in nerve tissue engineering.

PC12 cells seeded onto TCP and electrospun mats were allowed to settle for 24 h, prior to being treated with differentiation media containing 50 ng/mL of NGF. After 4 days of incubation in differentiation media, PC12 cells were immunostained for protein ß-III tubulin, a key neural differentiation marker, which is associated with the neurite cytoskeleton and DAPI, a nucleic acid stain. The PC12 cells were stained positively for ß-III tubulin on TCP and electrospun PCL–PPy mats (Fig. 10), indicating that both surfaces supported PC12 differentiation. Additionally, neuronal outgrowth is clearly visible from cells within these populations, and neurites of up to 150 μm were observed. Cell clustering behaviours, typical for PC12 cells, were
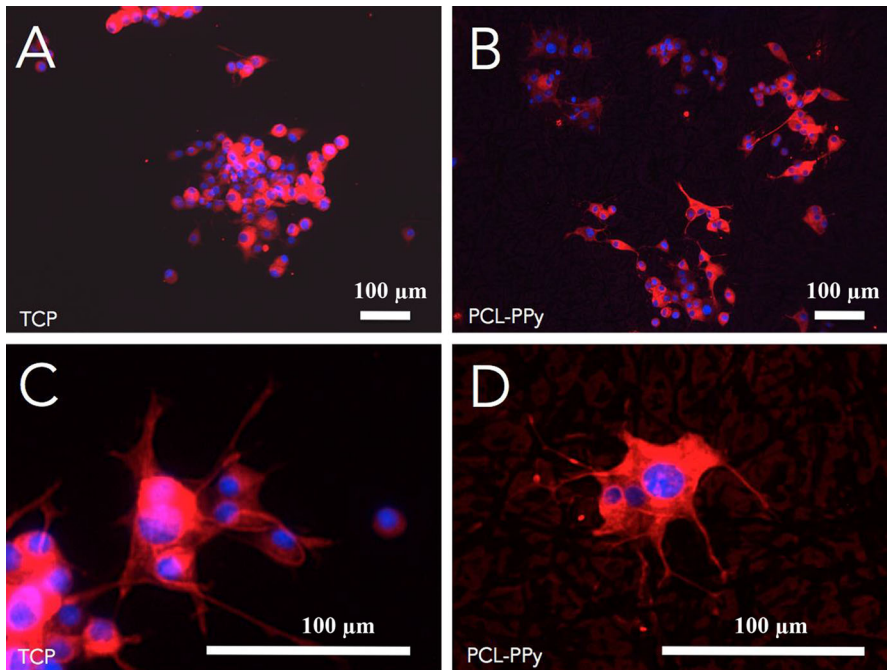
Fig. 10 Low and high magnification images of PC12 cells after 4 days of differentiation on TCP (**a** and **c**) and PCL–PPy (**b** and **d**). Cells have been stained for ß-III tubulin (*red*) and DAPI (*blue*). (Color figure online)

evident in both systems and limited the ability to quantify neural outgrowth by image analysis tools. These results demonstrated that PCL–PPy mats can support the proliferation and differentiation of PC12 cells. The interaction of PC12 cells on the PCL and PCL–PPy fibres is shown in Fig. 11. It was observed that the cells had flattened and spread across a number of fibres after 24 h of culture. Visual observation of the cells both by fluorescent microscopy and electron microscopy
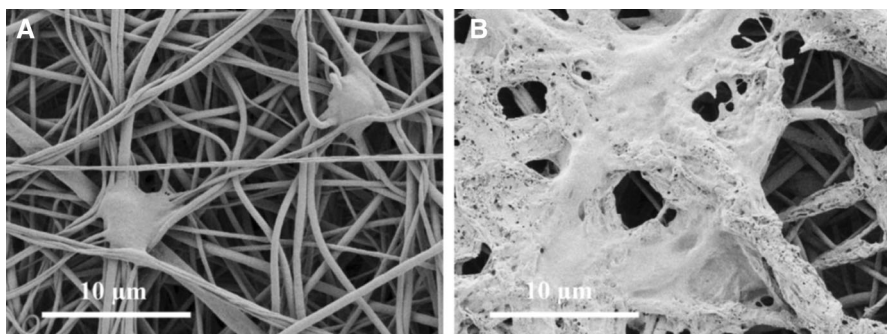

Fig. 11 SEM images of PC12 cells on samples. Image **b** shows that cells can find better features for attachment on the coated fibres compared to PCL fibres without coating in image **a**. **a** PC12 cells on uncoated PCL sample, **b** PC12 cells on PCL–PPy sample

revealed a more widespread proliferation of the cells on the PCL–PPy scaffolds. The analysed SEM images showed that the area covered by PC12 cells were 9 and 55 % for PCL and PCL–PPy samples, respectively. This large difference suggests that the features or conductivity of scaffold number 2 has increased the cell attachment or proliferation of the PC12 cells compared to PCL without coating.

Conclusion

Biodegradable polymeric scaffolds that are electrically conducting are attractive for tissue engineering, particularly for nerve tissue regeneration. The electrospun PCL nanofibres in this study (diameter: 0.87 ± 0.42 µm) was electrosprayed with Fe.pTS and coated by PPy in a vapour-phase polymerisation process. The electrospun fibre mats had a porosity of approximately 92 % and mechanically robust with elongation at break higher than 450 % in needle direction and Young's modulus higher than 4.6 MPa in perpendicular direction, which meets the requirements of tissue engineering scaffolds. The PCL-PPy mats changed the non-conductive PCL fibres to have electrical conductivities ranging from 1.3 to 1.9 S/cm. The selected sample number 2 for biological assessment with 54 % PPy coating spread over the PCL fibres showed that the electrically conducting PCL–PPy mats have excellent biocompatibility and supported the growth of neural-like cells. PC12 cells covered 55 % of the surface of the coated scaffold where only 9 % of the PCL without coating was covered by cells. Taken together, the results obtained can promote design of scaffold interfaces for nerve or muscle tissue engineering.

References

1. M. Okamoto, B. John, Prog. Polym. Sci. **38**, 10–11 (2013)
2. J. De Boer, C. Van Blitterswijk, P. Thomsen, J. Hubbell, R. Cancedda, J.D. de Bruijn, A. Lindahl, J. Sohier, D.F. Williams, *Tissue Engineering* (Elsevier Science, Amsterdam, 2008)
3. M.A. Woodruff, D.W. Hutmacher, Prog. Polym. Sci. **35**(10), 1217 (2010)
4. A. Tamayol, M. Akbari, N. Annabi, A. Paul, A. Khademhosseini, D. Juncker, Biotechnol. Adv. **31**, 669–687 (2012)
5. A. Cipitria, A. Skelton, T. Dargaville, P. Dalton, D. Hutmacher, J. Mater. Chem. **21**(26), 9419 (2011)
6. T.K. Dash, V.B. Konkimalla, J. Control. Release **158**(1), 15 (2012)
7. W.-J. Li, R. Tuli, C. Okafor, A. Derfoul, K.G. Danielson, D.J. Hall, R.S. Tuan, Biomaterials **26**(6), 599 (2005)
8. H.S. Kim, H.S. Yoo, Nanomedicine **9**(4), 517 (2014)
9. A. Subramanian, U.M. Krishnan, S. Sethuraman, Ann. Biomed. Eng. **40**(10), 2098 (2012)
10. M.P. Prabhakaran, L. Ghasemi-Mobarakeh, S. Ramakrishna, J. Nanosci. Nanotechnol. **11**(4), 3039 (2011)
11. L. Binan, A. Ajji, G. De Crescenzo, M. Jolicoeur, Stem Cell Rev. Rep. **10**(1), 44 (2014)
12. J.G. Hardy, J.Y. Lee, C.E. Schmidt, Curr. Opin. Biotechnol. **24**(5), 847 (2013)
13. L. Ghasemi-Mobarakeh, M.P. Prabhakaran, M. Morshed, M.-H. Nasr-Esfahani, S. Ramakrishna, Biomaterials **29**(34), 4532 (2008)

14. M. Naebe, T. Lin, X. Wang, *Carbon Nanotubes Reinforced Electrospun Polymer Nanofibres* (InTech, Vienna, 2010)
15. H. Bagheri, Z. Ayazi, M. Naderi, Anal. Chim. Acta **767**, 1 (2013)
16. H. Deng, L. Lin, M. Ji, S. Zhang, M. Yang, Q. Fu, Prog. Polym. Sci. **39**(4), 627 (2014)
17. M. Naebe, T. Lin, L. Feng, L. Dai, A. Abramson, V. Prakash, X. Wang, *Nanoscience and Nanotechnology for Chemical and Biological Defense* (American Chemical Society, Washington, DC, 2009), pp. 39–58
18. R. Balint, N.J. Cassidy, S.H. Cartmell, Acta Biomater. **10**, 2341–2353 (2014)
19. G.G. Wallace, *Conductive Electroactive Polymers: Intelligent Polymer Systems*, 3rd edn. (CRC Press, Boca Raton, 2009)
20. J. Wang, H.E. Naguib and A. Bazylak, in *SPIE Smart Structures and Materials + Nondestructive Evaluation and Health Monitoring* (International Society for Optics and Photonics, 2012), pp. 83420F–83413
21. A. Laforgue, L. Robitaille, Chem. Mater. **22**(8), 2474 (2010)
22. J. Foroughi, G.M. Spinks, G.G. Wallace, P.G. Whitten, Synth. Met. **158**, 3–4 (2008)
23. N.K. Guimard, N. Gomez, C.E. Schmidt, Prog. Polym. Sci. (Oxford) **32**, 8–9 (2007)
24. Y.D. Kim, J.H. Kim, Colloid Polym. Sci. **286**, 6–7 (2008)
25. G. Jin, K. Li, Mater. Sci. Eng., C (2014). doi:10.1016/j.msec.2014.06.004
26. X. Liu, J. Chen, K.J. Gilmore, M.J. Higgins, Y. Liu, G.G. Wallace, J. Biomed. Mater. Res., Part A **94A**(4), 1004 (2010)
27. B. Guo, L. Glavas, A.-C. Albertsson, Prog. Polym. Sci. **38**(9), 1263 (2013)
28. H. Cui, Y. Liu, M. Deng, X. Pang, P. Zhang, X. Wang, X. Chen, Y. Wei, Biomacromolecules **13**(9), 2881 (2012)
29. D. Mawad, E. Stewart, D.L. Officer, T. Romeo, P. Wagner, K. Wagner, G.G. Wallace, Adv. Funct. Mater. **22**(13), 2692 (2012)
30. D. Kai, M.P. Prabhakaran, G. Jin, S. Ramakrishna, J. Biomed. Mater. Res., Part A **99 A**(3), 376 (2011)
31. L. Ghasemi-Mobarakeh, M.P. Prabhakaran, M. Morshed, M.H. Nasr-Esfahani, H. Baharvand, S. Kiani, S.S. Al-Deyab, S. Ramakrishna, J. Tissue Eng. Regener. Med. **5**(4), e17 (2011)
32. P. Moroder, M.B. Runge, H. Wang, T. Ruesink, L. Lu, R.J. Spinner, A.J. Windebank, M.J. Yaszemski, Acta Biomater. **7**(3), 944 (2011)
33. J. Zhang, K. Qiu, B. Sun, J. Fang, K. Zhang, H. Ei-Hamshary, S.S. Al-Deyab, X. Mo, J. Mater. Chem. B **2**(45), 7945 (2014)
34. S. Meng, Tissue Eng. Regener. Med. **11**(4), (2014)
35. J.Y. Lee, C.A. Bashur, A.S. Goldstein, C.E. Schmidt, Biomaterials **30**(26), 4325 (2009)
36. A.O.H. Tavanai, M. Morshed. Polym. Adv. Technol. **23**(9), (2012)
37. A.J. Patil, S.C. Deogaonkar, J. Appl. Polym. Sci. **125**(2), 844 (2012)
38. S.J. Kim, D.H. Jang, W.H. Park, B.-M. Min, Polymer **51**(6), 1320 (2010)
39. F. Yang, R. Murugan, S. Wang, S. Ramakrishna, Biomaterials **26**(15), 2603 (2005)
40. C.S. Wong, E. Nuhiji, A. Sutti, G. Keating, X. Liu, M. Kirkland, X. Wang, Text. Res. J. **82**(13), 1371 (2012)
41. S.J. Park, B.-K. Lee, M.H. Na, D.S. Kim, Acta Biomater. **9**, 7719–7726 (2013)
42. P. Danilevicius, L. Georgiadi, C.J. Pateman, F. Claeyssens, M. Chatzinikolaidou, M. Farsari, Appl. Surf. Sci. **336**, 2 (2015)
43. K. Rezwan, Q. Chen, J. Blaker, A.R. Boccaccini, Biomaterials **27**(18), 3413 (2006)
44. A.R. Nectow, K.G. Marra, D.L. Kaplan, Tissue Eng. Part B Rev. **18**(1), 40 (2012)
45. R.H.W. Funk, T. Monsees, N. Özkucur, Prog. Histochem. Cytochem. **43**(4), 177 (2009)
46. A. Ndreu, L. Nikkola, H. Ylikauppilar, N. Ashammakhi, V. Hasirci, Nanomedicine **3**, 1 (2008)
47. Q. Lian, D. Li, L. Zhu, Z. Jin, Jixie Gongcheng Xuebao/J. Mech. Eng. **50**, 4 (2014)
48. A.J. Bauer, Y. Wu, B. Li, Macromol. Biosci. **16**, 5 (2016)
49. A.J. Bauer, T. Zeng, J. Liu, C. Uthaisar, B. Li, Macromol. Rapid Commun. **35**(7), 1524 (2014)
50. C.-L. Pai, M.C. Boyce, G.C. Rutledge, Macromolecules **42**(6), 2102 (2009)
51. R. Ravichandran, S. Sundarrajan, J.R. Venugopal, S. Mukherjee, S. Ramakrishna, Macromol. Biosci. **12**(3), 286 (2012)
52. W.-J. Li, R.L. Mauck, J.A. Cooper, X. Yuan, R.S. Tuan, J. Biomech. **40**(8), 1686 (2007)
53. E. Pektok, B. Nottelet, J.-C. Tille, R. Gurny, A. Kalangos, M. Moeller, B.H. Walpoth, Circulation **118**(24), 2563 (2008)